ISSN No. 2321-2705 | DOI: 10.51244/IJRSI |Volume XII Issue VII July 2025

Geochemical Characters of Leptynites from Melur, Madurai District, Tamil Nadu, South India

K. Vijayaragavan, A. Thirunavukkarasu*, S. Rakkiannan, C. Sakthivel

Department of Geology, Periyar University, Salem, Tamil Nadu, India

***Corresponding author:**

DOI: https://doi.org/10.51244/IJRSI.2025.120700119

Received: 08 July 2025; Accepted: 12 July 2025; Published: 06 August 2025

ABSTRACT

Leptynites occur with minor bands of basic granulites, charnockites, calcsilicate rocks, quartzites and khondalites in the Melur area in the Southern granulite terrane (SGT), India. Interbedded grey and cream leptynite types are distinguished based on field relations and geochemistry. They are paragneisses (khondalites) comprising quartz-felspar-sillimanite gneiss, quartz-felspar-garnet-sillimanite gneiss and their variants; charnockite series consisting of pyroxene granulites (basic) and charnockites (acidic); granites, pegmatites and aplites; and dolerites. Charnockites, granites and dolerites are successfully emplaced into the basement rocks' interbanded paragneiss and pyroxene granulites. Leptynite is noticed at the contact of paragenesis and charnockite. Based on whole-rock geochemistry, it is evident that both charnockite patches and host leptynites are isochemical. The adamellite composition, per-aluminous nature with positive Europium anomaly of host leptynite and charnockite patches, suggests their co-genetic relation. Higher values of (La/Yb)N and (Gd/Lu)N of leptynites indicate the highly fractionated HREE pattern of leptynites. The total REE, LREE/HREE and Eu-Eu∗ data indicate their derivation from the post-Archaean granodioritic upper crust comprising large proportions of impure greywackes with K-rich granitic components.

Keywords: Petrology, Geochemistry, Leptynites, Melur, Madurai

INTRODUCTION

The Madurai Block is regarded as a composite entity formed by the accretion of magmatic arcs that developed through prolonged subduction events, along with intermingled oceanic and supracrustal lithologies, followed by regional metamorphism during the late Neoproterozoic-Cambrian orogeny (Santosh et al., 2009b). According to (Santosh et al. 2003, 2009, 2011, 2012, 2013a,b; Braun and Appel, 2006; Kröner et al. 2012; Plavsa et al. 2012; and Collins et al. 2013), the Southern Granulite Terrain (SGT) is a collage of crustal blocks, including the Madurai Block, with ages spanning Neoarchean, Paleoproterozoic, and Neoproterozoic periods. These blocks are interpreted to have formed in active convergent margin settings, specifically suprasubduction zones and arc magmatic environments, as suggested by (Santosh et al. 2009; Yellappa et al. 2012; Teale et al. 2011; Ram Mohan et al. 2013; and Santosh et al. 2012, 2013a,b). The Madurai Block's northern boundary is the Palghat-Cauvery Shear Zone, which is considered a late Neoproterozoic collision zone and the trace of the Gondwana suture formed during the closure of the Mozambique Ocean, based on the work of (Collins et al. 2007 and Santosh et al. 2009). To the south, it is bounded by the Achankovil Shear Zone, which has been interpreted variably as a suture or a rift (Santosh et al. 2009 and Collins et al. 2013). Recent studies by (Ghosh et al. 2004; Plavsa et al. 2012; and Brandt et al. 2014) have indicated that the Madurai Block comprises an association of Archean to Neoproterozoic granite and charnockite, along with gneiss, calc granulite, and quartzite. According to (GSI, 2009), India, Madagascar, Sri Lanka, Antarctica, and western Australia are considered to have been part of East Gondwanaland until their break-up and dispersal in Mesozoic times (Yoshida, 1995; Rogers et al., 1995). They state that a better understanding of the tectonomagmatic and metamorphic events recorded in these crustal fragments during Precambrian times is crucial for reconstructing the East Gondwana assembly.

ISSN No. 2321-2705 | DOI: 10.51244/IJRSI |Volume XII Issue VII July 2025

The Melur area in the Madurai district, part of India's Peninsular Gneissic Complex (PGC), hosts leptynite interlayered with minor bands of basic Granulites, charnockite, calcsilicate rocks, quartzites, and khondalite. This study systematically investigates the petrography, mineral chemistry, and phase equilibria of schists and gneisses from two distinct metamorphic zones within this region. The garnet metamorphic zone is characterized by mica schist, garnet-bearing mica schist, felsic leptynite, and interlayered plagioclase amphibolite. In contrast, the sillimanite metamorphic zone comprises garnet-bearing biotite mica schist, sillimanite-bearing biotite-plagioclase gneiss, and felsic leptynite. Garnet crystals from the garnet metamorphic zone exhibit growth zoning, showing increased almandine and pyrope content and decreased spessartine from their core to their rim. Conversely, garnet within the sillimanite metamorphic zone displays a nearly homogeneous composition. Petrographic and geochemical evidence strongly suggests a metasedimentary origin for the leptynite/ pink granite in the Melur area, supported by: (a) their intercalation with talc-granulites, anhydrous aluminous minerals (such as almandine + sillimanite + cordierite ± sapphirine ± spinel), and quartzites; (b) their higher Na_2O content; (c) chondrite-normalized Rare Earth Element (REE) patterns of leptynite (47.6-238.2) and pink granite (71.8- 673.4) Leptynite/ pink granite; and (d) molecular $Al_2O_3/(CaO + Na_2O + K_2O)$ values greater than 1.1 (Chappel and White, 1974). The study aims to study the field, petrography, and geochemistry of granite/ leptynite rock from the Melur area.

Geology of the study area

The Madurai Block (Fig. 1) is split into two by a NE–SW trending feature known as the Karur–Kamban–Painavu–Trichur (KKPT) lineament (Ghosh et al., 2004). This lineament marks an isotopic boundary with Archaean crust lying to the northwest and Proterozoic crust preserved to the south and east (Bhaskar Rao et al., 2003; Ghosh et al., 2004; Plavsa et al., submitted for publication; Tomson et al., 2006). The KKPT also marks the surface expression of a series of south-dipping reflectors prominent in the region's deep reflection seismic survey (Rajendra Prasad et al., 2007). The Proterozoic metasedimentary rocks in the Madurai Block commonly yield zircons with ages from 2.6 to 1.8 Ga (Collins et al., 2007b; Sato et al., 2011), although occasional older Mesoarchaean and Mesoproterozoic zircons have also been reported (Collins et al., 2007b; Sato et al., 2011). Collins et al. (2007b) suggested that these might correlate with the Itremo Group of central Madagascar and that the Madurai Block might form a southern continuation of the intra-East African Orogen continent Azania (Collins et al., in press; Collins and Pisarevsky, 2005). Others have disputed this and instead interpret the metasedimentary rocks of the Madurai Block as a metamorphosed passive margin to the Dharwar craton of India (Bhaskar Rao et al., 2003; Ghosh et al., 2004). The Melur area has witnessed major crustal anatexis leading to the generation of a large volume of garnetiferous quartz-felspathic rock (leptynite) which occurs as a 15km long ENE-WSW/ E-W (Fig.1) trending linear belt between Kilaiyur in the west and Keelavalavu-Purakuttu Malai in the east within the gneiss/meta-sedimentary sequence. Quartzite occurs as discontinuous bands and lenses within this rock. The white rock contains K-feldspar, Plagioclase and quartz with minor biotite. Pink colored garnet is ubiquitously developed in this rock. Presence of enclaves/schlieren of garnet-biotite gneiss suggests that the quartzo-feldspathic rock could be the anatectic product of the metasedimentary protoliths during intense migmatisation. The garnet-bearing quartz-felspathic rock is being extensively quarried for dimension stone because of its pure white colour with pink dots of garnet. The area exhibits rocks of granulitic facies represented by the khondalite and charnockite belonging to the Eastern Ghat Super group. Several thin bands of calc granulite, ranging in size from 25 m to 2 km with a width of about a few centimetres to 20-30 m, are seen east and west of Karungalakkudi. Around Malampatti, the calc granulite forms wider bands. The increase in thickness of these bands in the area may be due to repeated folding. Garnetiferous sillimanite gneiss (metapelites) occurs as lenses in garnetiferous granulite of the Kilaiyur/ Keelavalavu area. Sulphide mineralization is also noticed in metapelites. Metapelite is a disadvantage factor in getting dimensional stone. This rock formation is primarily composed of a supracrustal assemblage of quartz and feldspar (± sillimanite ± graphite ± garnet ± magnetite), intricately interbanded with calc-silicate rocks and dolomite, as well as garnetiferous gneiss or schist, all occurring within a large expanse of biotite gneiss (± garnet). Broadly, the rocks around Melur are classified into the khondalite and charnockite groups. The khondalite group in this area mainly consists of calc-granulite/crystalline limestone and garnetiferous sillimanite gneiss, with minor quartzite bands. The charnockite group, on the other hand, includes acid to intermediate charnockite with subordinate two-pyroxene granulite.

ISSN No. 2321-2705 | DOI: 10.51244/IJRSI |Volume XII Issue VII July 2025

Subsequent migmatization and reconstitution of both rock groups led to the formation of grey-colored migmatite, encompassing hornblende-biotite gneiss, garnet-biotite gneiss, and garnetiferous quartzo-feldspathic granulite. Intrusions of younger pink granite and pink pegmatoidal granite further transformed parts of the grey migmatite into pink migmatitic gneiss and pink augen gneiss. Specifically, the white garnetiferous quartzo-feldspathic granulite east of Melur is interpreted as reconstituted garnetiferous sillimanite gneiss. In contrast, the well-developed pink augen gneiss near Tiruchunai is attributed to the blastic growth of pink potash feldspar augen within the grey biotite gneiss. The area's final stage of intrusive activity is represented by numerous minor pegmatite and quartz veins.

MATERIALS AND METHODS

Five fresh rock chips of medium and coarse-grained Leptynite/ pink granite samples are prepared for thin sections based on the textural arrangement of minerals. Chip samples are sent to Continental Instruments (Lab Crystals, Thin Section Preparations, Lucknow) to make thin sections. For each location, samples are collected in the Melur leptynite/ pink granite for analyzing the crystallization texture. Textural analysis and petrographic properties are studied under the Leica DM2700 P (Leica Application Suite) petrological microscope at the Department of Geology, Periyar University, India. Samples are pulverised to 63µ using steel and agate mortars. The pulverised 17 samples are sent to the Activation Laboratory Limited, Canada, for Litho geochemistry and Whole Rock Analysis. The samples are analysed under the package code of 4 Litho (WRA+ICP). The package needs 5g of the pulverised sample to pass 95% through 105 microns (µm). The most aggressive fusion technique employs a lithium metaborate/tetraborate fusion. Fusion is performed by a robot at Actlabs.

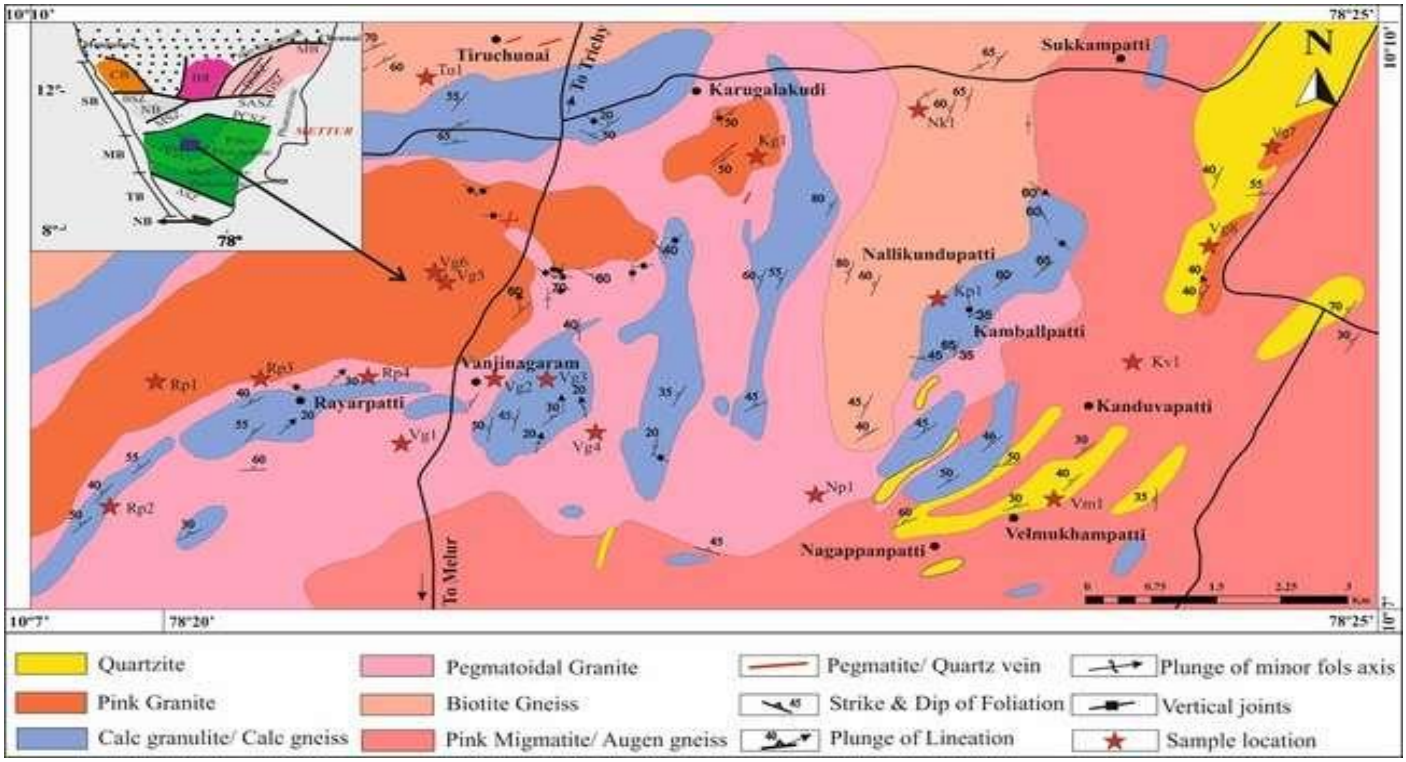

Figure 1: Geology and structural map of the study area (after Krishnan, 1989).

The resulting molten bead is rapidly digested in a weak nitric acid solution. The fusion ensures that the entire sample is dissolved. With this attack, major oxides including SiO_2, refractory minerals (i.e. Zircon, sphene, monazite, chromite, gahnite, etc.), REE and other high field strength elements are put into solution. High sulphide-bearing rocks may require different treatment, but can still be adequately analyzed. The analysis is by ICP-OES and ICP-MS. Eu determinations are semi-quantitative in samples having extremely high Ba concentrations (> 5 %). The samples are run for major oxides and selected trace elements (4B) on an ICP. Calibration is performed using 14 prepared USGS and CANMET-certified reference materials.

ISSN No. 2321-2705 | DOI: 10.51244/IJRSI |Volume XII Issue VII July 2025

Field Relationship

Leptynite

Leptynite rocks are typically light-colored, appearing in white, grey, or pinkish tones due to the predominance of quartz and feldspar. They are fine-to medium-grained with a granoblastic texture that indicates equigranular interlocking mineral grains formed under high-grade metamorphism (Fig.2). Essential minerals include quartz, alkali feldspar (microcline/orthoclase), and Plagioclase. In contrast, accessory minerals such as garnet, biotite, sillimanite, or graphite may also be present, depending on the protolith composition and metamorphic conditions. The texture is generally granoblastic or lepidoblastic, with occasional weak foliation or lineation resulting from directed stress, and faint compositional banding caused by mineral segregation during deformation. Leptynite often forms smooth, rounded outcrops, with surfaces appearing slightly exfoliated or polished due to weathering of quartz-rich layers. The Leptynite (Kashmir White) is a product of the remelting of the pre-existing country rock garnetiferous sillimanite gneiss and pegmatite vein intruded in granite rock at Royarpatti and Vanjinagaram (Fig.2a). This image (likely the one showing a light-colored rock with visible minerals) illustrates the Kashmir White granite. As previously explained, this granite formed from partially melting garnetiferous sillimanite gneiss. The image also depicts a pegmatite vein (a coarse-grained igneous intrusion) cutting through the granite, indicating a later phase of magmatic activity.

The presence of both features in one image provides insights into the complex geological history of the area. Pegmatite enclave within granite at Sukampatti area: These images (likely showing variations of a coarse-grained rock within a finer-grained rock) would show pegmatite enclaves (inclusions) within a larger granite body, specifically in the Sukampatti area. Pegmatites are characterized by their exceptionally large crystals, and these images would highlight the contrast between the pegmatite and the surrounding granite. The variations in the images (Fig.2b-d) might show different sizes, shapes, or mineral compositions of the pegmatite enclaves. Presence of garnet like allanite produced within pink pegmatoidal granite, Karugalakudi (Fig. 2 g): This image (likely depicting a pinkish rock with dark crystals) shows a pink pegmatoidal granite containing garnet-like crystals, which are likely allanite. Allanite is a sorosilicate mineral, similar to garnet. Pegmatoidal granite is a very coarse-grained variety of granite. The pink colour is due to the presence of potassium feldspar. This image highlights the mineralogical diversity found within pegmatites and granites.

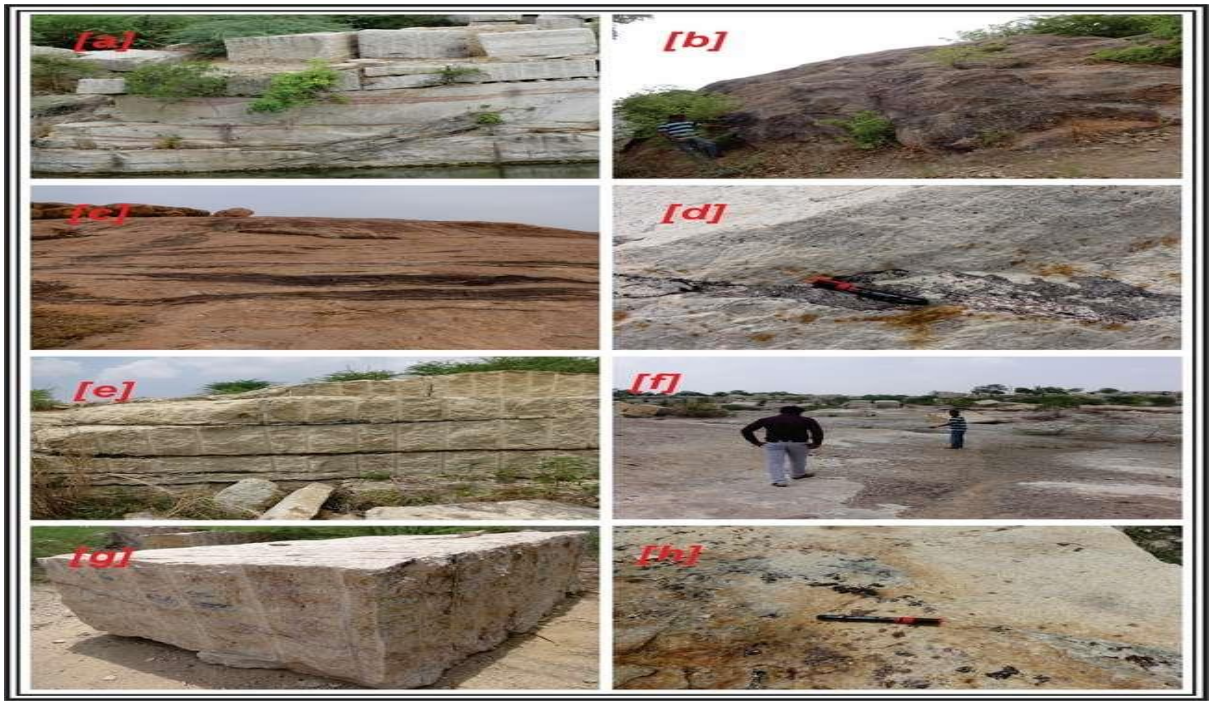

Figure 2: Field photographs of (a) Leptynite (Kashmir White) is a product of remelting of the pre-existing country rock garnetiferous sillimanite gneiss and pegmatite vein intruded in granite rock at Royarpatti and Vanjinagaram, (b-d) pegmatite enclave within granite at Sukampatti area, (g) Presence of garnet like allanite

ISSN No. 2321-2705 | DOI: 10.51244/IJRSI |Volume XII Issue VII July 2025

produced within pink pegmatoidal granite, Karugalakudi, (e-f,h) granite rock exposed at Vanjinagaram area, Quartzo - Feldspathic Granite (leptynite) near Vanjinagaram area, Melur Taluk.

Granite rock exposed at Vanjinagaram area, Quartzo - Feldspathic Granite (leptynite) near Vanjinagaram area, Melur Taluk (Fig.2e-f, h): These images (likely showing various exposures of granite) depict granite outcrops in the Vanjinagaram area. They may also include examples of leptynite, a fine-grained to medium-grained metamorphic rock derived from granite, characterized by a granoblastic texture (equigranular crystals). The images might show variations in the granite's texture, colour, and degree of weathering.

Pink Granite

This Melur area provides a close view of a coarse-grained igneous rock, likely a granite or a similar plutonic rock (Fig.3a). The interlocking crystals of different minerals are visible. The white or light-colored minerals are predominantly feldspars, such as Plagioclase and Orthoclase. The glassy, gray to translucent grains are quartz. The darker specks and grains are likely biotite or hornblende, ferromagnesian minerals. The phaneritic texture, where all the crystals are large enough to be seen without magnification, indicates that this rock cooled slowly beneath the Earth's surface, allowing ample time for crystal growth. The variations in colour and mineral distribution can provide clues about the specific composition and the conditions under which the rock formed. Royarpatti and Vanjinagram showcases a heavily fractured and weathered outcrop of what appears to be a felsic igneous rock, possibly another type of granite or a related rock like granodiorite (Fig.3b). The dominant reddish-pink hue suggests the presence of iron oxides, which could be a result of the weathering of iron-bearing minerals within the rock over time. The extensive network of joints and fractures indicates that the rock has been subjected to significant tectonic stresses or freeze-thaw cycles, leading to its fragmentation. The loose, broken pieces at the base illustrate the ongoing physical weathering and erosion process. This Kamballpatti area captures a section of a rock quarry, revealing distinct horizontal layers or bedding planes within the rock mass (Fig.3c). These layers could represent different deposition stages if the rock is sedimentary, or they might be joints or fractures that formed parallel to the surface due to pressure release as overlying material was removed. The dark, vertical stains are likely caused by water percolating through the rock and dissolving or depositing minerals, such as iron or manganese oxides. The presence of vegetation growing on the ledges indicates some degree of weathering and the accumulation of soil or sediment in these areas. The water body at the base suggests that the quarry may have intersected the water table or is collecting rainwater.

The Tiruchunai area presents a relatively smooth, exposed surface of a metamorphic rock, possibly a gneiss or a migmatite. The mottled appearance with irregular bands and patches of pink and gray suggests a history of high-temperature and high-pressure metamorphism, which has caused the segregation of different minerals into distinct layers or lenses (Fig.3d). The subtle textural variations might reflect the original rock type and the intensity of the metamorphic processes. The lighter patches could represent areas enriched in felsic minerals (quartz and feldspar), while the darker areas might be richer in mafic minerals (biotite, hornblende). The Karugalakudi area shows a geological contact between two distinct rock types (Fig.3e).

Figure 3: Field photographs showing in (a) Leptynite (Kashmir White) is a product of remelting of the pre-existing country rock garnetiferous sillimanite gneiss, (b) quartzo feldspathic granite at Melur, (c) pegmatite

ISSN No. 2321-2705 | DOI: 10.51244/IJRSI |Volume XII Issue VII July 2025

enclave within granite at Vanjinagaram area, (d and h) The mottled appearance with irregular bands and patches of pink and gray suggests a history of high-temperature and high-pressure metamorphism, (e-g) Quartzo Feldspathic Granite (Leptynite) near Vanjinagaram area, Melur.

The rock on the left contains pegmatite veins, which are very coarse-grained intrusive igneous rocks characterized by exceptionally large crystals. These veins often form during the late stages of magma crystallization when volatile-rich fluids allow for rapid crystal growth. The rock on the right is labelled as containing garnet, indicating a metamorphic rock that has experienced conditions suitable for forming these characteristic red to brownish-red, roughly spherical crystals. The sharp boundary between the pegmatite veins and the garnet-bearing rock suggests an intrusive relationship, where the pegmatitic magma intruded into and cross-cut the pre-existing metamorphic rock. This is a closer view of the garnet-bearing metamorphic rock seen in the previous image. The dark, reddish-brown, roughly equidimensional crystals of garnet are visible embedded within a finer-grained matrix at the Sukkampatti area (Fig.3f). Garnet is a common index mineral in metamorphic rocks, and its presence can provide valuable information about the temperature and pressure conditions under which the rock formed. The surrounding matrix likely consists of other metamorphic minerals such as quartz, feldspar, and possibly mica. The overall texture and mineral assemblage suggest that this rock has undergone significant recrystallization due to metamorphism. This Vanjinagaram area shows another view of a rock quarry, possibly the same one in image (Fig.3c, g), highlighting further details of the rock structure. The presence of multiple horizontal layers or joints is again evident. There also appears to be a dipping feature in the lower part of the exposed rock face, which could be a fault, a fold, or an inclined sedimentary layer. The varying colours and textures within the different layers suggest potential changes in the rock composition or weathering intensity. Vegetation grows on the upper surfaces and along some of the fractures, indicating areas where soil and moisture have accumulated. A close-up of a pink granite that has been intruded by biotite veins in the Nagappanpatti area (Fig.3h) shows the pink colour of the granite due to the presence of potassium feldspar. The biotite veins are thin, dark, wavy features that cut across the granite. Biotite is a dark-colored mica mineral rich in iron and magnesium. These veins likely formed when a later pulse of magma or hydrothermal fluids, enriched in biotite-forming elements, intruded into the already solidified granite through fractures. The pen provides a scale for the features observed. This image illustrates a common geological process where older rocks are cross-cut by younger intrusive features.

Petrography

Leptynite

The leptynites in the study area display several interesting textural features, including interlocking quartz and feldspar, graphic intergrowths of Plagioclase and quartz, perthitic intergrowths between albite and K-feldspar, and intergrowths of garnet and biotite. In addition to these major minerals, minor constituents such as ilmenite and spinel are present, with ilmenite often found as inclusions within garnet. Some leptynite samples contain garnet porphyroblasts enclosing orthopyroxene and sillimanite (Fig.4). The granite in the area is composed primarily of K-feldspar (~35%), Plagioclase (~30%), quartz (~30%), and biotite (~5%), with accessory phases (<1%) including apatite, Zircon, allanite, opaques, muscovite, sericite, epidote, chlorite, calcite, titanite, garnet, and tourmaline (Table 1). Microscopically, leptynite exhibits an inequigranular, medium- to coarse-grained texture dominated by quartz, plagioclase feldspars (white oligoclase), string-like and stringlet-like perthite, microcline, and minor amounts of rounded to subrounded garnet and biotite mica; accessory minerals include Zircon and muscovite mica. Myrmekitic intergrowths of quartz and plagioclase feldspars and alteration of plagioclase feldspars to zoisite/kaolin are observed in places. Conversely, a higher proportion of microcline feldspar relative to plagioclase feldspars is associated with a more common occurrence of pink colouration in the leptynite deposit. The leptynite of Melur shows evidence of garnet rusting, bent twin lamellae in plagioclase feldspar (likely due to later deformation), and alteration of garnet to biotite, which probably contributes to iron staining upon weathering. Host leptynites are characterized by abundant plagioclase and alkali feldspar in roughly equal proportions, and myrmekitic intergrowths of quartz and feldspars are common. Biotite, garnet, and ilmenite are also present, with biotite distributed arbitrarily throughout the rock and small ilmenite inclusions common. Granoblastic texture is a prevalent feature in these leptynites. In some locations, small patches of pelitic assemblages (sillimanite – biotite – garnet – feldspar – quartz + ilmenite) occur as xenoliths within the leptynite (Fig.3).

ISSN No. 2321-2705 | DOI: 10.51244/IJRSI |Volume XII Issue VII July 2025

Microscopic description of leptynite (Kashmir white)

Garnet

Garnets occurred as coarse xenoblasts of anhedral structure. They are usually fractured due to high stress within the rocks, which are later filled with iron leaching. They are poikiloblastic, including spinel, biotite, Plagioclase, quartz and magnetite. In some sections of leptynite, garnet porphyroblasts are deformed and filled with sillimanite, biotite and orthopyroxene (Fig.4a-c). Spinel occurs as a rhombic structure and was found as an inclusion in garnet and ilmenite (Fig. 4d). Under plane polarised light, spinel is green in colour, non-pleochroic and has no cleavage, while under cross-nichol, the mineral is black, hence isotropic. Spinel inclusion indicated the prograde metamorphic process (Fig. 4e-f).

Biotite

Biotites are subhedral with corroded surfaces. They are pleochroic from yellowish brown to dark brown. They are found as inclusions within garnet, and those developed in garnet show no particular cleavage planes. They have formed assemblages with garnet, Plagioclase, K-feldspar and quartz. This textural relation suggested that biotite and quartz react to form garnet and potash feldspar (Fig. 4a). Zircon in biotite is widespread. Petrography also indicated the effects of radioactivity on biotite, which are indicated by dark radioactive halos within the minerals. Biotite was also included within K-feldspar (Fig. 4c). In some sections, biotite and quartz are included in garnet porphyroblast, which is again surrounded by biotite, Orthoclase, and quartz (Fig. 4e). The textural relation might suggest the following reaction: (Biotite + quartz = Garnet + K-feldspar).

Plagioclase

Plagioclases were medium to coarse, colourless, nonpleochroic minerals with anhedral to subhedral structure. They have shown lamellar twinning, sometimes in two sets perpendicular to one another, and developed perthitic intergrowth (Fig. 4). The Ab-An content in Plagioclase of leptynite in the study area varied from Ab21-28 and An2-14. Plagioclases in some sections are altered into clay minerals undergoing sericitization. Sericite is grungy-looking, fine-grained stuff that commonly replaces Plagioclase. Their birefringence is irregular and generally low because they comprise tiny crystals.

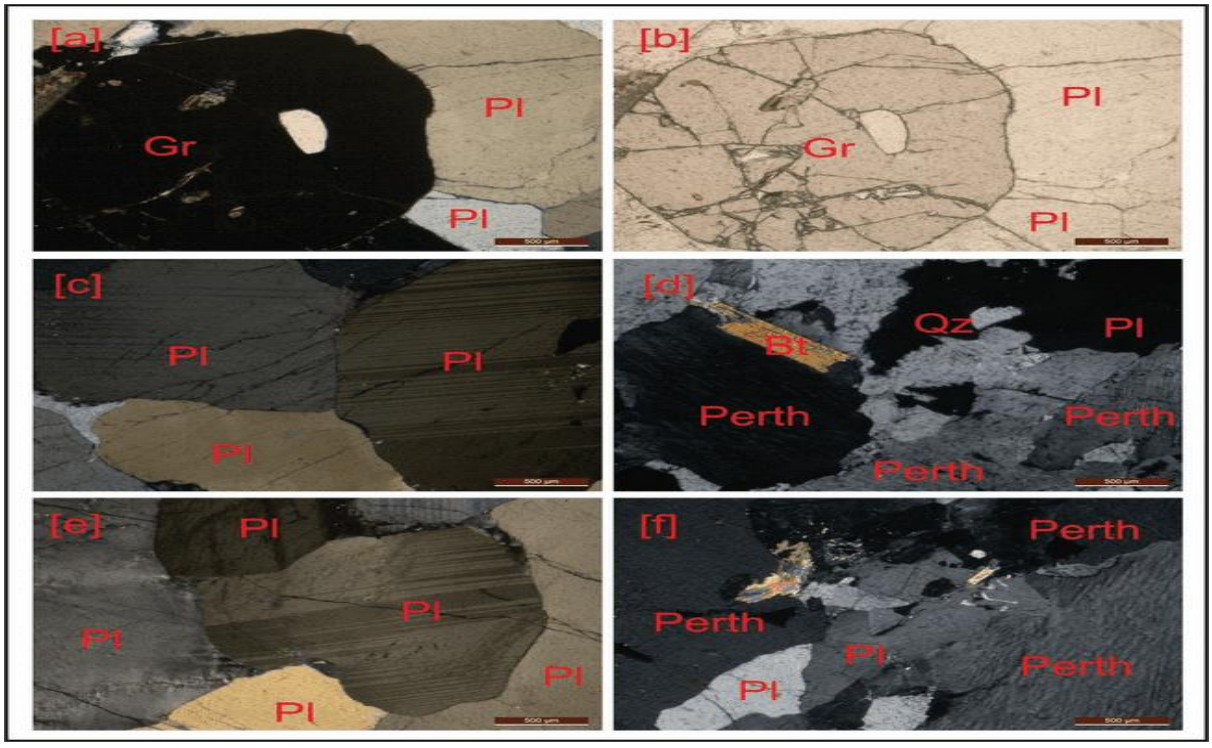

Figure 4: The (a-f) Photomicrographs showing important textural features include interlocking texture between quartz and feldspar, graphic intergrowth of Plagioclase and quartz and intergrowth of garnet and

ISSN No. 2321-2705 | DOI: 10.51244/IJRSI |Volume XII Issue VII July 2025

biotite; Garnets occurred as coarse xenoblasts of anhedral structure; Biotite also occurred as an inclusion within K-feldspar; They have shown lamellar twinning which are sometimes in two sets perpendicular to one another and they developed perthitic intergrowth.

K-feldspar

The potash-feldspar in the present leptynite is found as microcline. They occurred as anhedral to subhedral minerals. They have formed assemblages with Plagioclase, biotite and quartz surrounding xenoblasts of garnet crystal. They have displayed polysynthetic twinning (Fig. 4d). The perthitic intergrowth of albite and microcline is very common. Sometimes, microcline includes biotite (Fig. 4a).

Quartz

Quartz occurred in an anhedral form and was colourless under plane polarised light. They commonly occur as inclusions within garnet, K-feldspar and biotite (Fig. 4). They have displayed wavy extinction, which might indicate origin by syntectonic crystallization.

Sillimanite

Sillimanites occurred as inclusions in garnet porphyroblasts. They are colourless and found in a needle-shaped form under plane polarised light. They are observed in between the cracks of deformed garnet porphyroblasts. They found small prismatic forms of orthopyroxene within garnet and small biotite flakes (Fig. 4 b & e). The mineral association might indicate the following mineral reaction: (Garnet + K-feldspar +H_2O = biotite + sillimanite + quartz).

Pink Granite

This granite shows coarse-to-medium-grained hypidiomorphic equigranular to porphyritic texture with euhedral K-feldspar phenocrysts embedded in an eugranitic matrix. Most of the K feldspar phenocrysts have microcline twinning with well-developed linear perthite exsolution lamellae and grade imperceptibly into smaller polygonal grains due to the recrystallization in deformed samples. Myrmekitic colonies are abundant along the grain boundaries of K-feldspar in some samples (Fig. 5). Plagioclase, mostly unzoned and poikilitic, shows sericite and saussurite alteration in a few grains. Quartz often forms an interlocking network with feldspars, and at places is strained with the incipient formation of sub-grains. Aggregates of biotite laths occur interstitially, having inclusions of apatite, Zircon, and opaques, and are partially altered to chlorite and epidote at a few places. The secondary muscovite is occasionally intergrown with biotite or occurs as irregular grains in Plagioclase. Angular to sub-rounded grains of garnet occur around biotite and contain tiny inclusions of biotite itself.

The pink granite consists of approximately. 40% quartz, 55% K-feldspar and Plagioclase, with the former dominating the latter and the remaining primarily comprised of biotite and minor hornblende. The accessories (<1%) include Zircon, titanite, allanite, fluorite, apatite, epidote, sericite, chlorite, rutile and opaques (Table 1). Most K-feldspar shows simple twinning, and some mantle the plagioclase grains. Exsolution textures like microperthite, occasionally mesoperthite and micrographic intergrowth are very common. The abundance of the ferromagnesian mineral is more variable in this granite than in others, as some samples of this granite do not have any appreciable amount of biotite or hornblende. Such variation in mineral content could be the result of fractional crystallization. The accessories (<1%) include Zircon, titanite, allanite, fluorite, apatite, epidote, sericite, chlorite, rutile and opaques. Most K-feldspar shows simple twinning, and some mantle the plagioclase grains. Exsolution textures like microperthite, occasionally mesoperthite and micrographic intergrowth are very common. The abundance of the ferromagnesian mineral is more variable in this granite than in others, as some samples of this granite do not have any appreciable amount of biotite or hornblende. Such variation in mineral content could be the result of fractional crystallization.

ISSN No. 2321-2705 | DOI: 10.51244/IJRSI |Volume XII Issue VII July 2025

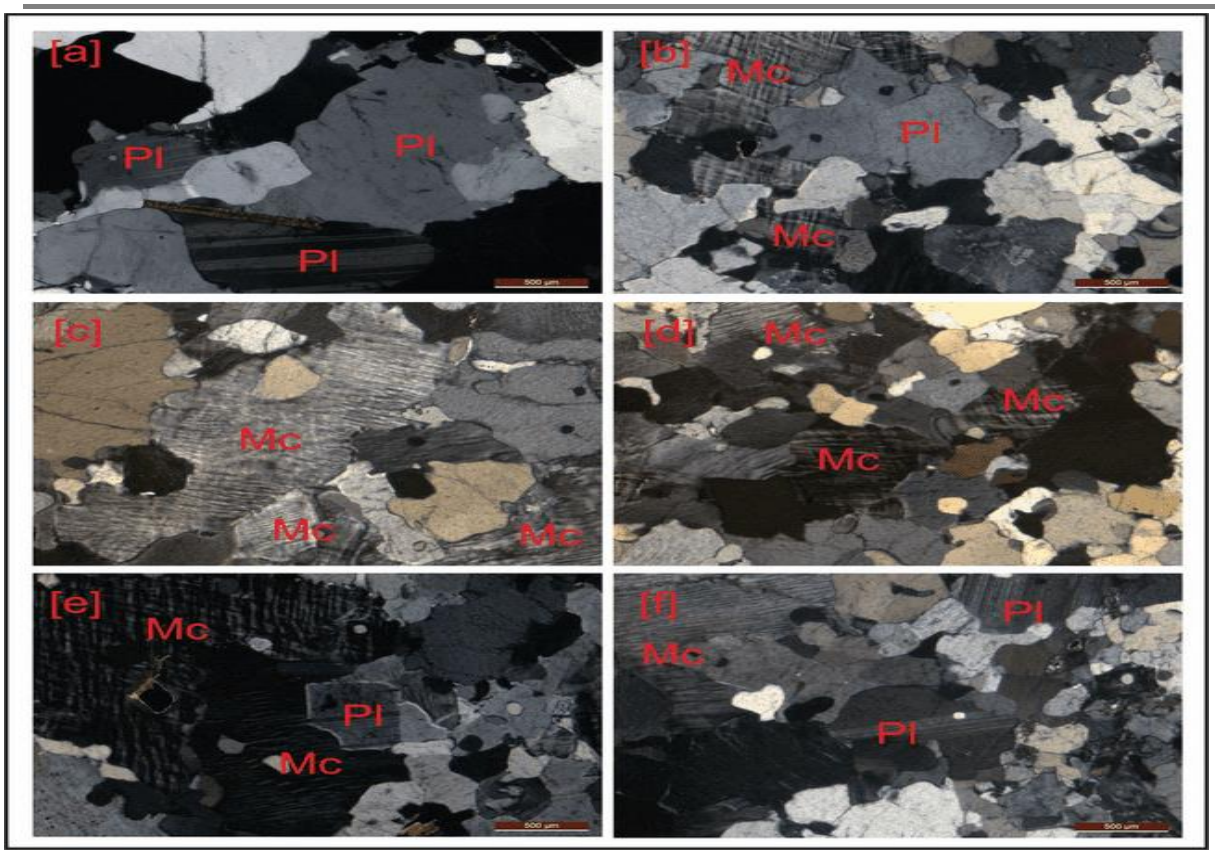

Figure 5: The Photomicrographs showing (a-f) pink granite rock the microcline perthites show patch- and braided-perthites and are commonly surrounded and traversed by rims and veinlets of micro granulated and recrystallized quartz respectively; The plagioclases, particularly the larger crystals show varying degrees of sericitization and saussuritization; Large crystals of microcline exhibit characteristic grid (cross-hatched) twinning and sometimes take a significant percentage of the stage.

Microscopic description of minerals

Microcline

The microcline perthites show patch- and braided-perthites and are commonly surrounded and traversed by rims and veinlets of microgranulated and recrystallized quartz, respectively. Slight sericitization of the K-feldspars is observed. Some of the patch perthites look very much like replacement perthites.

Sodic Plagioclase

Sodic plagioclases (Ab-An12) occur as large and small discrete grains and exsolved phases in the potassium feldspar. The plagioclases, particularly the larger crystals, show varying degrees of sericitization and saussuritization (Fig. 5). The reaction involves loss of potassium and calcium by the feldspars and probably accounts for the dominance of sodic Plagioclase in samples with high epidote mineral contents; (ii) a lesser amount occurs as discrete grains with no apparent relationship to the alteration of feldspars or any other mineral. Plagioclase, while in contact with microcline, develops an albitic rim and occasional development of myrmekite. The clustered aggregate with its crystallographic arrangement resembles Plagioclase, formed early in a crystallizing silicate melt.

K- Feldspar

K-feldspar has an average size ranging between 8 and 12 mm (Fig.5). Large crystals of microcline exhibit characteristic grid (cross-hatched) twinning and sometimes take a significant percentage of the stage. K-feldspar crystals are albite and are elongate, and Plagioclase exhibits well-formed polysynthetic twins (Fig. 5). Orthoclase appears euhedral and exhibits recognizable Carlsbad twinning with well-defined edges.

ISSN No. 2321-2705 | DOI: 10.51244/IJRSI |Volume XII Issue VII July 2025

Quartz

Quartz is primarily interstitial to the feldspars, but some occur in the granulated and recrystallized rims and veinlets around and within the feldspars, while some occur simply as inclusions in the feldspars (Fig. 5). Quartz grains are subhedral in shape and occur as clear crystals with a white colour. Few tiny quartz grains resembling those crystallized during the stress of ductile shear are observed; such grains exhibit translational fabrics and wavy extinction. Quartz is also of two generations; the latter replaces plagioclase feldspar and occurs in interstitial spaces.

Epidote

Epidote minerals are present in almost all sections and vary in amount from accessory to major component, sometimes exceeding the typical ferromagnesian mineral (Fig. 5).

Biotite

Biotite flakes have been chloritized to different degrees and are seldom found fresh. They have a greenish colour with green and yellow pleochroic colours. Muscovite occurs as discrete flakes (including those formed as by-products of epidotization) and as an alteration product of the feldspars. Biotite occurs as large brown crystals (Fig. 5a-b &d). Biotite is a stretched mineral with randomly oriented laths of diagnostic light to dark-brown colour.

Hornblende

Hornblende appears as sub-angular and elongate masses with pleochroism typically pale brown to dark brown, while biotite occurs as large plates and groundmass minerals. Smaller grains of quartz and hornblende form the supporting minerals in an interlocking structure.

Opaque minerals

Iron oxide, sphene, Zircon, allanite and apatite are accessory minerals. Garnet occurs in amounts varying between the minor and accessory components (Fig. 5). It is commonly poikiloblastic, including quartz, biotite, and hornblende. It may be fractured and elongated parallel to the direction of gneissosity in the rock.

Table 1. Textural and mineralogical characters of granite and leptynites of the Melur area

Type	Modal Mineralogy		Texture
Granite		Average	
	Quartz	32.1	Pink and white colour in fresh outcrop, fine to medium-grained, granoblastic rock. Stringlet perthites are remarkable. Bands and layers are conspicuous with well-defined streaky elongation of garnet and biotites. Reaction zones of silimanite and garnet are recorded between spinel and quartz.
	Plagioclase	27.3	
	K-Feldspar	29.2	
	Biotite	5.0	
	Spinel	2.5	
	Zircon	0.7	
	Apatite	0.6	
	Opaques	2.6	

ISSN No. 2321-2705 | DOI: 10.51244/IJRSI |Volume XII Issue VII July 2025

Leptynite	Quartz	28.9	Mostly medium-grained, Leptynite (Kashmir white) exhibits a spotted appearance due to garnet porphyoblasts in coarse varieties. Patchy perthites and myrmekites are prominent.
	Plagioclase	16.9	
	K-Feldspar	38.4	
	Garnet	10.3	
	Biotite	2.8	
	Zircon	0.7	
	Apatite	0.4	
	Opaques	1.6	

Whole rock geochemistry

Major elements

The chemical data of leptynite/ pink granite and Niggli and normative values (Q, Or, Ab) are listed in Table 2. The chemical analyses of leptynite/ pink granite show variations in almost all major elements, reflecting the mineral phases of those particular samples. SiO_2 is >60% in all analyzed samples. The leptynite/ pink granite varies from 56 to 73.4%, averaging 67.4%. $A1_2O_3$ values commonly approach > 15% in the leptynite samples, and it rises to 16% in the leptynite/ pink granite due to higher sillimanite and spine1 concentrations (Fig.6 and 7). The averages of total Fe and MgO of leptynites (0.4% to 2.8%) are at higher levels than the pink granite (1.2% to 6.3%). The concentration levels of CaO, Na_2O, MnO and P_2O_5 do not show much variation among grey and cream leptynite samples. The K_2O content of leptynite samples (1.0-4.5 = 2%) exceeds pink granite (1.0-4.0 = 2.2%). A characteristic difference is the higher K_2O content than Na_2O in all analyzed samples, except that the local segregation of plagioclase feldspar is prominent in the sample. K-feldspars mainly cause the higher K_2O content, in general, in the leptynite samples in the mineral assemblage. The abundance of K-feldspar may be related to intra-crustal melting of post-Archaean upper crust, followed by production of K-rich granitic components.

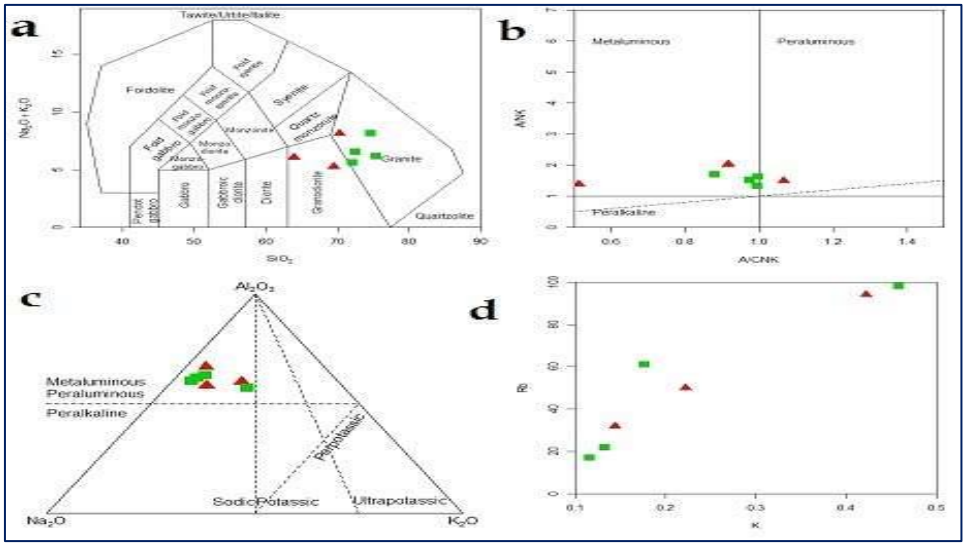

Figure 6: a) TAS; b) Discrimination diagram of Alumina saturation index Shand (1943) with the relative source of rocks; c) Maniar and Piccoli (1989) showing peraluminous nature for leptynite/ pink granite; d) K-Rb relationship diagram of leptynites.

ISSN No. 2321-2705 | DOI: 10.51244/IJRSI |Volume XII Issue VII July 2025

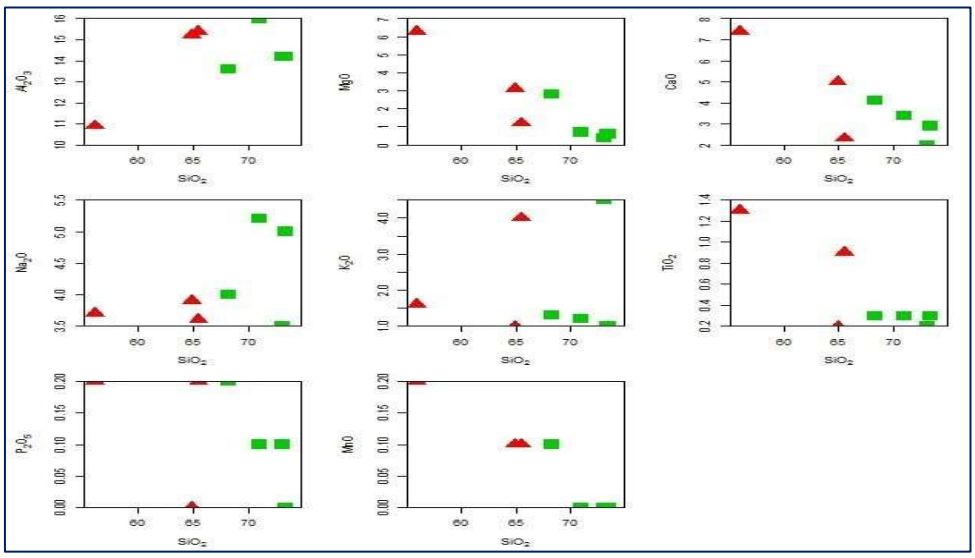

Figure 7: Major oxide elements vs. Si_2O (wt.%) variation diagrams of the Melur leptynite/ pink granite.

Trace elements

The trace element data (Rb, Sr, Ba, Zr, Cr, Co, V, Ni, Cu, SC, Ta, Hf) and inter-elemental ratios of grey and cream leptynites are presented in Table 2.

Large-ion lithophile elements (LILE)

Table 2 shows that the leptynite samples are characterized by relatively high concentrations and substantial variations of large-ion lithophile elements (LILE). The Rb content of leptynites varies from 17 to 98 ppm and is comparable to that of pink granite (32- 94 ppm). The Sr content of analyzed samples does not show much variation. The Ba content of leptynite ranges from 219 to 1244 ppm, averaging at 569 ppm, whereas the pink granite variety shows relatively high concentration, ranging from 166 to 1210 ppm at an average of 663 ppm. A Significant positive correlation between K and Rb (Fig. 7d and 8). The ratio varies from a minimum of 17 to a maximum of 98, due to the erratic behaviour of Rb. The overall K-Rb ratios indicate a severe depletion of both K and Rb on the one hand, while enrichment of both of these elements exhibited K-Rb ratios around 250. Shaw (1968) found that the K-Rb ratio in normal upper crustal rocks averages 250, but there was a slight tendency to increase with decreasing Rb content. A negative tendency was observed between K and Ba. The variable K-Rb and K-Ba ratios may reflect the provenance differences, mineral fractionation during deposition or metamorphic effects. The Zr content does not show much variation between leptynite (143 ppm) and pink granite (177 ppm) samples, and the concentration could be contributed by accessory zircon.

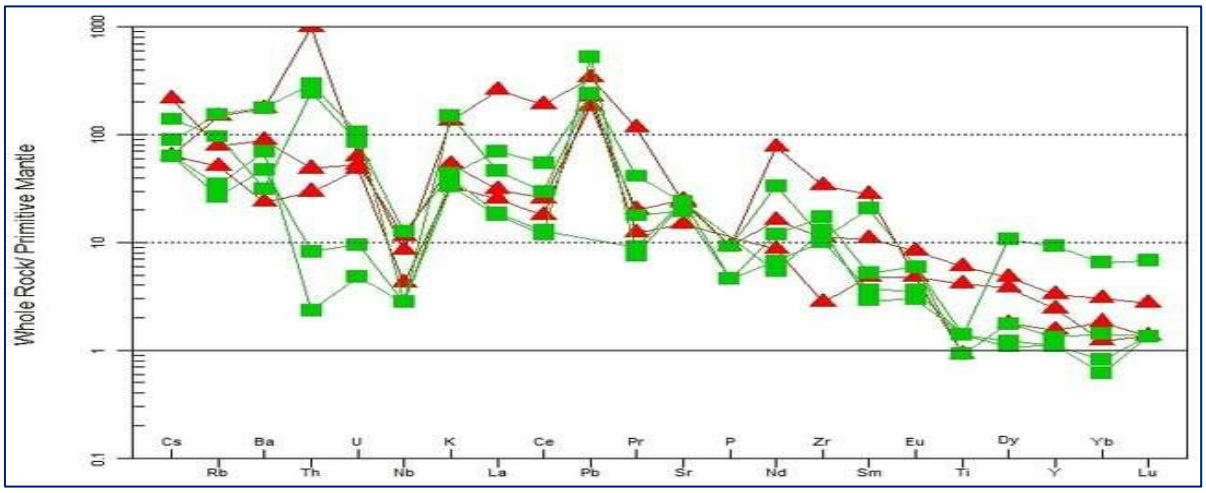

Figure 8. Trace element concentration of leptynite/ pink granite from the Melur area, Madurai. Normalization values are from Sun and McDonough (1989). (a) Primitive mantle normalized spider diagram of rocks.

ISSN No. 2321-2705 | DOI: 10.51244/IJRSI |Volume XII Issue VII July 2025

Ferromagnesium trace elements

Ferromagnesium trace elements show significant variations between grey and cream leptynites (Table 2). The concentrations of these elements are found at higher levels in leptynites (Cr = 40-110 ppm, V = 27-45 ppm, Ni = 20-90 ppm, Co = 3-11 ppm, Sc = 2-19 ppm) and pink granite (Cr = 20-360 ppm, V = 166-1210 ppm, Ni = 30-230 ppm, Co = 12-49 ppm, Sc = 5-19 ppm). Ferromagnesium trace elements exhibit a positive trend with Fe_2O_3(t), particularly in the leptynite/ pink granite. The distribution of these elements shows a clear distinction between the leptynite/ pink granite varieties (Fig. 9). A close look at the analyzed data reveals that the leptynite/ pink granite samples show higher values of Si and LILE due to the abundance of quartz and K-feldspar. In contrast, the leptynite/ pink granite variety contains more Ti, Fe^{*+}, Fe^{3+}, Mg and ferromagnesium trace elements because of an appreciable presence of garnet, spinel, sillimanite and opaques.

Table 2: Major, Trace and REE data of leptynite/ pink granite of Melur area

Name	**VG51**	**VG6**	**VG2**	**VG63**	**VG69**	**VG34**	**VG38**
	Pink Granite			**Letynite**			
SiO_2	65.5	64.9	56.0	71.0	73.4	73.1	68.3
Al_2O_3	15.4	15.2	10.9	16.0	14.2	14.2	13.6
Fe_2O_3(T)	6.1	6.1	13.1	2.1	2.3	2.0	3.9
MnO	0.1	0.1	0.2	0.0	0.0	0.0	0.1
MgO	1.2	3.1	6.3	0.7	0.6	0.4	2.8
CaO	2.3	5.0	7.4	3.4	2.9	2.0	4.1
Na_2O	3.6	3.9	3.7	5.2	5.0	3.5	4.0
K_2O	4.0	1.0	1.6	1.2	1.0	4.5	1.3
TiO_2	0.9	0.2	1.3	0.3	0.3	0.2	0.3
P_2O_5	0.2	0.0	0.2	0.1	0.0	0.1	0.2
LOI	0.6	1.1	-0.2	0.4	0.9	0.4	0.8
Total	99.8	100.6	100.3	100.3	100.6	100.3	99.3
Sc	5.0	9.0	19.0	2.0	3.0	2.0	19.0
Be	< 1	1.0	2.0	< 1	< 1	1.0	2.0
V	143.0	52.0	234.0	27.0	31.0	32.0	45.0
Ba	1210.0	166.0	614.0	484.0	332.0	1244.0	219.0
Sr	494.0	310.0	516.0	508.0	495.0	412.0	505.0
Y	11.0	7.0	15.0	5.0	5.0	6.0	42.0
Zr	377.0	31.0	124.0	114.0	145.0	192.0	121.0
Cr	20.0	140.0	360.0	50.0	50.0	40.0	110.0

ISSN No. 2321-2705 | DOI: 10.51244/IJRSI |Volume XII Issue VII July 2025

Co	12.0	17.0	49.0	4.0	4.0	3.0	11.0
Ni	30.0	70.0	230.0	< 20	< 20	< 20	90.0
Cu	30.0	210.0	250.0	30.0	30.0	20.0	160.0
Zn	90.0	180.0	100.0	30.0	40.0	< 30	90.0
Ga	20.0	18.0	17.0	19.0	16.0	17.0	19.0
Ge	1.0	1.0	1.0	< 1	< 1	< 1	1.0
As	< 5	< 5	< 5	< 5	< 5	< 5	< 5
Rb	94.0	32.0	50.0	22.0	17.0	98.0	61.0
Nb	6.0	3.0	8.0	2.0	2.0	2.0	9.0
Mo	< 2	< 2	3.0	2.0	< 2	2.0	< 2
Ag	< 0.5	< 0.5	< 0.5	< 0.5	< 0.5	< 0.5	< 0.5
In	< 0.2	< 0.2	< 0.2	< 0.2	< 0.2	< 0.2	< 0.2
Sn	1.0	5.0	2.0	< 1	< 1	1.0	4.0
Sb	< 0.5	< 0.5	< 0.5	< 0.5	< 0.5	< 0.5	< 0.5
Cs	0.5	0.5	1.7	0.5	0.5	0.7	1.1
La	178.0	17.2	21.4	12.8	12.2	31.5	48.0
Ce	334.0	31.4	45.2	22.8	21.1	52.4	96.4
Pr	31.8	3.4	5.5	2.5	2.1	4.9	11.4
Nd	104.0	11.8	21.6	9.1	7.3	16.2	45.2
Sm	12.3	2.1	4.8	1.6	1.3	2.3	9.2
Eu	0.8	0.8	1.4	0.6	0.5	1.0	1.0
Gd	6.8	1.4	4.0	1.4	1.0	1.7	8.0
Tb	0.7	0.2	0.6	0.2	0.2	0.3	1.3
Dy	2.8	1.3	3.5	0.9	0.8	1.3	7.9
Ho	0.4	0.3	0.7	0.2	0.1	0.2	1.5
Er	1.0	0.8	1.7	0.4	0.4	0.7	4.1
Tm	0.1	0.1	0.2	0.1	0.1	0.1	0.5
Yb	0.6	0.9	1.5	0.3	0.4	0.7	3.2
Lu	0.1	0.1	0.2	0.1	0.1	0.1	0.5

ISSN No. 2321-2705 | DOI: 10.51244/IJRSI |Volume XII Issue VII July 2025

Hf	8.1	0.9	3.0	2.3	3.0	4.6	2.9
Ta	0.2	0.3	0.5	< 0.1	< 0.1	0.5	0.6
W	< 1	< 1	< 1	2.0	< 1	< 1	< 1
Tl	0.4	0.2	0.4	< 0.1	< 0.1	0.6	0.3
Pb	24.0	16.0	13.0	< 5	37.0	17.0	17.0
Bi	< 0.4	< 0.4	< 0.4	< 0.4	< 0.4	< 0.4	< 0.4
Th	84.3	2.5	4.1	0.2	0.7	24.9	21.0
U	1.3	1.0	1.1	0.1	0.2	2.2	1.8
Eu/Eu*	0.27	1.42	0.98	1.22	1.34	1.54	0.36
La/Yb	201.9	13.01	9.71	29.04	20.76	30.62	10.21
La/Sm	9.07	5.13	2.79	5.01	5.88	8.58	3.27
Ce/Yb	146.56	9.19	7.93	20.01	13.89	19.71	7.93
Ce/Sm	6.58	3.62	2.28	3.45	3.93	5.52	2.54
Eu/Yb	3.82	2.55	2.67	5.73	3.58	4.09	0.89
Total REE	673.4	71.8	112.3	53	47.6	113.4	238.2
Niggli							
si	336.7	276.9	196.4	356.4	411.1	420.9	319.6
al	46.647	38.213	22.52	47.328	46.866	48.173	37.496
fm	9.632	20.08	33.527	5.239	5.01	3.433	19.928
c	12.67	22.85	27.79	18.3	17.4	12.33	20.55
alk	31.05	18.85	16.15	29.14	30.72	36.05	22.022
k	0.422	0.144	0.222	0.132	0.116	0.458	0.176
mg	0.955	0.982	0.982	1	1	1	0.176
c/fm	3.435	0.64	3.42	1.133	1.26	0.86	1.05
ti	0.435	0	0.297	0.212	0	0.244	0.396
p	1.31	1.138	0.829	3.473	3.473	3.59	1.031
qz	112.5	101.504	31.744	139.846	188.258	176.639	131.497

ISSN No. 2321-2705 | DOI: 10.51244/IJRSI |Volume XII Issue VII July 2025

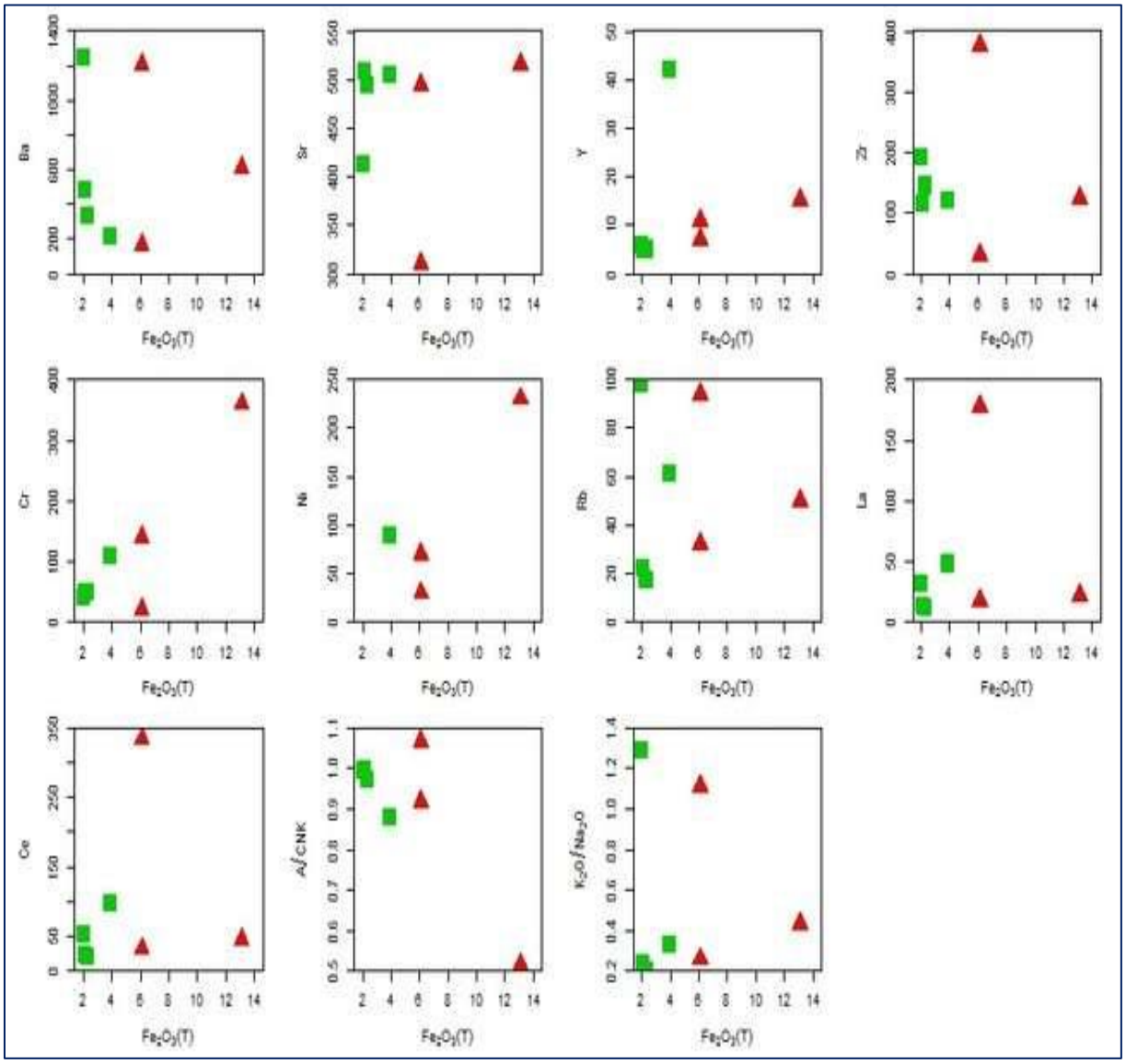

Figure 9: Plot of ferromagnesium trace elements (ppm) against total Fe_2O_3 (wt%) of leptynite/ pink granite.

Rare-Earth Elements (REE)

The REE data of the analyzed samples are given in Table 2, and these results, normalized to chondrites (Evenson et al., 1987), are plotted (Fig. 10). The REE data of leptynite/ pink granite display moderate to steep LREE patterns. However, the behaviour of HREE patterns of leptynite/ pink granite looks different (Fig. 10). The sample shows a distinct rise from Tb to Lu. The higher abundance of garnet and Zircon could explain the flat to enriched pattern of HREE. The depleted patterns of HREE of leptynite and pink granite are due to a lesser zircon concentration relative to garnet in those samples. The LREE enrichment and anomalous behaviour of Sm can be explained by the apatite and monazite distribution in the leptynite/ pink granite samples. The reason for Ce depletion is unknown, but it may be due to depositional and partly metamorphic conditions. The open ocean waters are known to be Ce depleted (Fleet, 1984; Humphris, 1984); hence, Ce depletion is more likely related to the depositional environment of the leptynite protolith. Leptynites are significant negative and positive (Fig. 10). Conversely, leptynite/ pink granite has negative Eu anomalies, except two samples (VG51, VG38) show positive anomalies. The positive anomalies in the analyzed samples could imply the occasional abundance of plagioclase feldspar. The Eu depletion in the leptynites may result from K-rich granitic components in the source. The REE patterns show strong fractionation with LaN-YbN values ranging from 10.21 to 30.62 for leptynite and 9.71-201.90 for pink granite. The total REE of leptynite (47.6- 238.2 ppm) is slightly higher than that of the pink granite variety (71.8-673.4 ppm).

ISSN No. 2321-2705 | DOI: 10.51244/IJRSI |Volume XII Issue VII July 2025

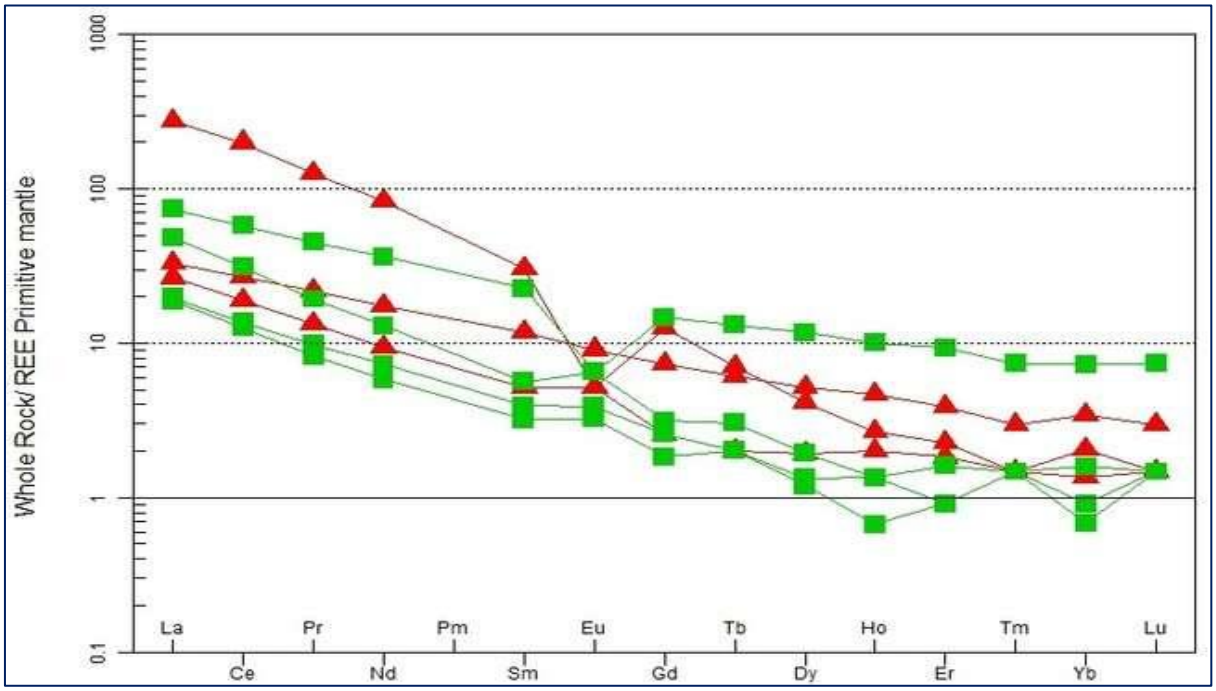

Figure 10. REE concentration of leptynite/ pink granite from the Melur area, Madurai. Normalization values are from Sun and Mc Donough (1989). (a) REE Primitive mantle normalized spider diagram of rocks.

DISCUSSION

The genesis of leptynite/ pink granite has an important bearing on understanding the deep crustal processes, particularly during Precambrian times. The leptynites were formed due to metamorphism of arenaceous with argillaceous mixtures (Bhattacharya, 1973) and rhyolite tuffs (Losert, 1971). Viswanathan (1969) opined that the leptynites are the sedimentary equivalents of greenstone belts. Partial melting of khondalite (Sen, 1987) and metapelite (Karmakar and Fukuoka, 1992) are suggested for the genesis of leptynites. According to Chacko et al. (1992), the leptynites (K-rich granulites) of the Kerala Khondalite Belt (KKB) were formed from arkosic, argillaceous and possibly felsic volcanic protoliths. The following field, petrographic and chemical evidences favour a metasedimentary origin for leptynite/ pink granite of the Melur area: (a) intercalations of talc-granulites and quartzites, (b) presence of anhydrous aluminous minerals (almandine garnet + sillimanite + cordierite &- sapphirine f spinel), (c) higher K_2O-Na_2O, and (d) molecular $A1_2O_3$ &CaO + Na_2O+ K_2O) values (Table 2) greater than 1.1 (Chappel and White, 1974). The Niggli values of leptynite / pink granite samples when represented in 100 mg-c-(al-alk) and (al-alk) vs c diagrams (Fig. 6) fall within the greywacke field. The leptynites generally have higher ferromagnesium trace element contents than pink granite (Table 2). Paragneisses' relatively low Cr and Ni contents differ from most Archaean greywackes and pelites, suggesting a felsic granitoid-volcanic predominant source (Condie et al., 1991).

The REE pattern has proven to be particularly useful in giving information on the source rocks of metasediments. REE are fractionated very little and are immobile during sedimentary processes (Chaudhuri and Cullers, 1979; McLennan, 1982; Fleet, 1984). The REE in metamorphic rocks are unaffected up to the upper amphibolite facies regional metamorphism (Taylor and McLennan, 1985) and sometimes little mobile during metamorphism (Muecke et al., 1979; McLennan, 1982; Humphris, 1984). The average REE distribution in elastic sediments has often been assumed to display the average content of the upper continental crust (McLennan, 1982). According to Taylor and McLennan (1981), the sedimentary rocks of continental crust show a negative Eu anomaly for the upper crust, a positive anomaly for the lower crust and no Eu anomaly for the whole crust. The leptynites derived from elastic sediments (impure greywackes) are potentially useful for estimating the REE composition of a portion of the upper continental crust. In the Proterozoic era, upper crustal rocks were highly differentiated and granodioritic in composition; in Archaean times, they were more mafic and less differentiated with lower LREE/HREE ratios.

ISSN No. 2321-2705 | DOI: 10.51244/IJRSI |Volume XII Issue VII July 2025

The common sedimentary rocks of the post-Archaean, including sandstones, mudstones and carbonates, on average show a significant and constant depletion in Eu, whereas Archaean counterparts show an Eu-Eu* ratio without deviation from 1.0 (McLennan, 1982; Taylor and McLennan, 1985). The REE pattern is also very important in providing information on the provenance of elastic sediments (McLennan, 1982). Primitive mantle -normalized REE data of leptynite/ pink granite are characterized by moderate to steep LREE with flat to enriched and depleted HREE patterns (Fig. 10). The Eu anomaly is variable. However, on average, there is no anomaly for leptynite and a negative anomaly for pink granite. Such REE patterns resemble felsic volcanics in Archaean terrains (O'Nions and Pankrust, 1978; Jahn and Sun, 1979). The REE data and Eu-Eu* factor (leptynite 0.36-1.54; pink granite 0.27-1.42) of leptynite/ pink granite are broadly comparable with that of greywacke (Okeke et al., 1983) and post-Archaean upper crust (Taylor and McLennan, 1985). High LREE/HREE (47.6-238.2) with Eu-Eu* depletion factor (0.27-1.54), low Na_2O, CaO contents and high K_2O & Na_2O ratios (Table 2) suggest K-rich granitic components in the source.

CONCLUSION

The leptynite in the Melur area originated from crustal anatexis and intense migmatization of metasedimentary rocks under granulitic facies conditions. Its mineral composition (quartz, feldspar, garnet) and granoblastic texture suggest slow cooling and partial melting at high temperatures. Textural features, such as perthitic textures, polysynthetic twinning in Plagioclase, and garnet equilibrium growth further indicate slow cooling and moderate to high-pressure dynamic metamorphism. The presence of equilibrium garnet, biotite, and quartz, coupled with the observed textures, strongly supports the region's partial melting and high-grade metamorphism. Studying the Melur leptynite is crucial for understanding the area's metamorphic history and tectonic evolution, offering insights into the high-temperature and pressure conditions associated with regional tectonic processes and crustal thickening. The K-rich granitic components may have formed through intracrustal melting of a post-Archaean upper crust containing sediments. The consistently Eu-depleted pattern found in the KKB rocks suggests that the entire source region of KKB sediments underwent intracrustal melting processes necessary to produce an Eu-depleted (granitic) upper crust (Chacko et al., 1992). Archaean sedimentary rocks derived from felsic volcanics exhibit significant negative Eu anomalies (Boak et al., 1982; McLennan et al., 1984). The REE patterns of the leptynites closely align with those of greywacke and the post-Archaean upper crust (Fig. 7). Furthermore, the trace element distribution (low Cr and Ni) and REE distribution (particularly steeper LREE with flat HREE) suggest that the leptynites were derived from a heterogeneous post-Archaean granodioritic upper crust that included significant proportions of impure greywackes with K-rich granitic components, a conclusion supported by the chemical variations observed in the leptynite/pink granite.

ACKNOWLEDGEMENT

The authors thank the Department of Geology, Periyar University, Salem, India, for providing the DST-FIST-sponsored laboratory facilities. The authors also thank Activation Laboratories Ltd. (Actlabs), Canada, for analyzing the rock quickly, which helps the authors with publications.

REFERENCE

1. Amaldev, T., Santosh, M., Li, T., Baiju, K.R., Tsunogae, T., Satyanarayanan, M., 2016. Mesoarchean convergent margin processes and crustal evolution: petrologic, geochemical and Zircon U–Pb and Lu–Hf data from the Mercara Suture Zone, southern India. Gondwana Res. 37, 182–204.
2. Bartlett, J.M., Dougherty-Page, J.S., Harris, N.B.W., Hawkesworth, C.J., Santosh, M., 1998. The application of single zircon evaporation and model Nd ages to the interpretation of polymetamorphic terrains: an example from the Proterozoic mobile belt of south India. Contributions to Mineralogy and Petrology 131, 181– 195.
3. Bhaskar Rao, Y.J., Janardhan, A.S., Vijaya Kumar, T., Narayana, B.L., Dayal, A.M., Taylor, P.N., Chetty, T.R.K., 2003. Sm–Nd model ages and Rb–Sr isotope systematics of charnockites and gneisses across the Cauvery Shear Zone, southern India: implications for the Archaean-Neoproterozoic

ISSN No. 2321-2705 | DOI: 10.51244/IJRSI |Volume XII Issue VII July 2025

boundary in the southern granulite terrain. In: M. Ranmakrishnan (Ed.), Tectonics of Southern Granulite Terrain. Geological Society of India Memoir, vol. 50, pp. 297–317.
4. Bhattacharya C. (1973) Petrology of the leptynites and garnetiferous granite gneisses around Garbham, Srikakulam district, Andhra Pradesh. J. Geol. Sot. India U(2), 113-125.
5. Boak J. L., Dymek R. F. and Gromet L. P. C. (1982) Early crustal evolution: constraints from variable REE Patterns in metasedimentary rocks from the 3000 Ma Isua supracrustal belt, West Greenland (Abstract). Lunar Planer. Sci. XIII, 51-52.
6. Brown, M., Raith, M., 1996. First evidence of ultrahigh-temperature decompression from the granulite province of southern India. J. Geol. Soc. Lond. 153, 819–822.
7. Chacko T., Ravindra Kumar G. R., Meen J. K. and Rogers J. J. W. (1992) Geochemistry of high grade supracrustal rocks from the Kerala Khondalite Belt (KKB) and adjacent massif charnockites, South India. Precambrian Res. 55, 469-489.
8. Chappel B. W. and White A. J. R. (1974) Two contrasting granite types. Pac$c Geol. 8, 1973-1974.
9. Chaudhuri S. and Cullers R. L. (1979) The distribution of rare earth elements in deeply buried Gulf coast sediments. Chem. Geol. 24, 327-338.
10. Chetty, T.R.K., 1996. Proterozoic shear zones in southern granulite terrain, India. In: Santosh, M., Yoshida, M. (Eds.), Gondwana Research Group Memoir, vol. 3: The Archaean and Proterozoic Terrains in Southern India within East Gondwana, pp. 77–89.
11. Chetty, T.R.K., Bhaskar Rao, Y.J., 2006a. Constrictive deformation in transpressional regime: field evidence from the Cauvery Shear Zone, Southern Granulite Terrain, India. Journal of Structural Geology 28, 713–720.
12. Chetty, T.R.K., Bhaskar Rao, Y.J., 2006b. Strain pattern and deformational history in the eastern part of the Cauvery shear zone, southern India. Journal of Asian Earth Sciences 28, 46–54.
13. Clark, C., Collins, A.S., Kinny, P.D., Timms, N.E., Chetty, T.R.K., 2009. SHRIMP U–Pb age constraints on the age of charnockite magmatism and metamorphism in the Salem Block, southern India. Gondwana Res. 16, 27–36.
14. Clark, C., Collins, A.S., Santosh, M., Taylor, R., Wade, B.P., 2009. The P–T–t architecture of a Gondwanan suture: REE, U–Pb and Ti-in-zircon thermometric constraints from the Palghat Cauvery shear system, South India. Precambrian Research 174, 129–144.
15. Collerson K. D. (1975) Contrasting patterns of K/Rb distribution in Precambrian high grade metamorphic rocks from Central Australia. J. Geol. Sot. Australia 22, 145-158.
16. Collins, A.S., Clark, C., Plavsa, D., 2014. Peninsular India in Gondwana: the tectono thermal evolution of the Southern Granulite Terrain and its Gondwanan counterparts. Gondwana Res. 25, 190–203.
17. Collins, A.S., Clark, C., Sajeev, K., Santosh, M., Kelsey, D.E., Hand, M., 2007a. Passage through India: the Mozambique Ocean suture, high-pressure granulites and the Palghat-Cauvery shear zone system. Terra Nova 19, 141–147.
18. Collins, A.S., Pisarevsky, S.A., 2005. Amalgamating eastern Gondwana: the evolution of the Circum-Indian Orogens. Earth Science Reviews 71, 229–270.
19. Collins, A.S., Santosh, M., Braun, I., Clark, C., 2007b. Age and sedimentary provenance of the Southern Granulites, South India: U-Th-Pb SHRIMP secondary ion mass spectrometry. Precambrian Res. 155, 125–138.
20. Condie K. C., Wilks M., Rosen D. M. and Zlobin V. L. (1991) Geochemistry of metasediments from the Precambrian Hapscham series, eastern Anabar shield, Siberia. Precambrian Res. 50, 3747.
21. Cooray P. G. (1962) Charnockites and associated gneisses in the Precambrian of Ceylon. Q. J. Geol. Sot. London 118, 239273.
22. Drury, S.A., Harris, N.B.W., Holt, R.W., Reeves-Smith, J., Whiteman, R.T., 1984. Precambrian tectonics and crustal evolution in south India. Journal of Geology 92, 3–20.
23. Evenson N. M., Hamilton P. J. and O'Nions P. K. (1987) Rare earth element abundances in chondritic meteorites. Geochim. Cosmochim. Acta 42, 1199-1212.
24. Fleet A. J. (1984) Aquous and sedimentary geochemistry of rare earth elements. In Rare Earth Element Geochemistry (edited by Henderson P.), pp. 343-373. Elsevier, Amsterdam.
25. Geological Survey of India, 1995. Geological and Mineral Map of Tamil Nadu and Pondicherry, Bangalore.

ISSN No. 2321-2705 | DOI: 10.51244/IJRSI |Volume XII Issue VII July 2025

26. Ghosh, J.G., de Wit, M.J., Zartman, R.E., 2004. Age and tectonic evolution of Neoproterozoic ductile shear zones in the Southern Granulite Terrain of India, with implications for Gondwana studies. Tectonics 23 (TC3006). doi:10.1029/2002TC001444.
27. Halden N. M., Bowes D. R. and Dash B. (1982) Structural evolution of migmatites in granulite facies terrain: Precambrian crystalline complex of Angul, Orissa, India. Trans. R. Sot. Edinburgh Earth Sci. 73, 109-118.
28. Handke, M., Tucker, R.D., Ashwal, L.D., 1999. Neoproterozoic continental arc magmatism in west-central Madagascar. Geology 27, 351–354.
29. Harley S. L. (1985) Garnet-Orthopyroxene bearing granuhtes from Enderbyland, Antarctica: metamorphic pressure-temperature time evolution of the Archean Napier Complex. J. Petrol. 26, 819-856.
30. Harley S. L. (1988) Proterozoic granulites from the Rauer group, East Antarctica. I. Decompressional pressure-temperature paths deduced from mafic and felsic gneisses. J. Petrol. 29, 1059-1095.
31. Harris, N.B.W., Santosh, M., Taylor, P.N., 1994. Crustal evolution in south India: constraints from Nd isotopes. J. Geol. 102, 139–150.
32. Holland T. H. (1900) The charnockite series, a group of Archaean hypersthene rocks in Peninsular India. Mem. Geol. Surv. India 28, 119-249.
33. Humphris S. E. (1984) The mobility of the rare earth elements in the crust. In Rare Earth Element Geochemistry (edited by Henderson P.), pp. 317-342. Elsevier, Amsterdam.
34. Jahn B. and Sun S. S. (1979) Trace element and isotopic composition of Archaean greenstones. Phys. Chem. Earth 11, 597418.
35. Kapila Dahanayake and Jayasena H. A. H. (1983) General geology and petrology of some Precambrian crystalline rocks from the Vijayan complex of Sri Lanka. Precambrian Res. 19, 301-315.
36. Karmakar S. and Fukuoka M. (1992) Genesis of leptynites: evidence from Araku Valley, Eastern Ghats, India. Indian Minerals 46(3 & 4), 247-258. Leake B. E. (1964) The chemical distinction between ortho- and para-amphibolites. J. Petrol. 5, 238-254.
37. Kröner, A., Kehelpannala, K.V.W., Hegner, E., 2003. Ca. 750–1100 Ma magmatic events and Grenville-age deformation in Sri Lanka: relevance for Rodinia supercontinent formation and dispersal, and Gondwana amalgamation. Journal of Asian Earth Sciences 22, 279–300.
38. Losert J. (1971) On the volcanogenous origin of some Moldanubian leptynites. Krystallinikum 7, 61-84.
39. McLennan S. M. (1982) On the geochemical evolution of sedimentary rocks. Chem. Geol. 37, 335-350.
40. McLennan S. M. and Taylor S. R. (1984) Archaean sedimentary rocks and their relation to the composition of the Archaean continental crust. In Archaean Geochemistry (edited by Kroner A., Manson G. N. and Goodwin A. M.), pp. 47-74. Springer, Berlin.
41. McLennan S. M., Taylor S. R. and McGregor V. R. (1984) Geochemistry of Archaean sedimentary rocks from west Greenland. Geochim. Cosmochim. Acta 48, 1-13.
42. Muecke G. K., Pride C. and Sarkar P. (1979) Rare earth element geochemistry of regional metamorphic rocks. Phys. Chem. Earth 11, 449464.
43. Naganjaneyulu, K., Santosh, M., 2010. The Cambrian collisional suture of Gondwana in southern India: a geophysical appraisal. Journal of Geodynamics 50, 256–267.
44. Naganjaneyulu, K., Santosh, M., 2011. Crustal architecture beneath Madurai Block, southern India deduced from magnetotelluric studies: implications for subduction–accretion tectonics associated with Gondwana assembly. Journal of Asian Earth Sciences 40, 132–143.
45. Nance W. B. and Taylor S. R. (1976) Rare earth element patterns and crustal evolution. I: Australian Post Archaean sedimentary rocks. Geochim. Cosmochim. Acta 40, 1539-1551.
46. Naqvi S. M. and Rogers J. J. W. (1987) Precambrian Geology of India. Oxford University Press, Oxford, 223 pp.
47. Naqvi S. M., Sawkar R. H., Subba Rao D. V., Govil P. K. and Gnaneswara Rao T. (1988) Geology, geochemistry and tectonic setting of Archaean greywackes from Karnataka nucleus, India. Precambrian Res. 39, 193-216.
48. O'Nions R. K. and Pat&rust R. J. (1978) Early Archaean sedimentary rocks and geochemical evolution of the earth crust. Earth Planet. Sci. Lett. 38, 211-236.

ISSN No. 2321-2705 | DOI: 10.51244/IJRSI |Volume XII Issue VII July 2025

49. Okeke P. O., Borley G. D. and Watson J. (1983) A geochemical study of Lewisian meta-sedimentary granulites and gneisses in the Scourie-Laxaford area of the N-W Scotland. Mineral. Mag. 47,342.
50. Park A. F. and Dash B. (1984) Chamockite and related neosome development in the Eastern Ghats, Orissa, India; petrographic evidence. Trans. R. Sot. Edinburgh Earth Sci. 75, 341-352.
51. Plavsa, D., Collins, A.S., Foden, J.F., Kropinski, L., Santosh, M., Chetty, T.R.K., Clark, C., 2012. Delineating crustal domains in Peninsular India: age and chemistry of orthopyroxene-bearing felsic gneisses in the Madurai Block. Precambrian Res. 198- 199, 77–93.
52. Plavsa, D., Collins, A.S., Payne, J.L., Foden, J., Clark, C., Santosh, M., 2014. Detrital zircons in basement metasedimentary protoliths unveil the origins of sourthern India. Geol. Soc. Am. Bull. 126, 791–812.
53. Praveen, M.N., Santosh, M., Yang, Q.Y., Zhang, Z.C., Huang, H., Singanenjam, S., Sajinkumar, K.S., 2014. Zircon U–Pb geochronology and Hf isotope of felsic volcanics from Attappadi, southern India: implications for Neoarchean convergent margin tectonics. Gondwana Res. 26, 907–924.
54. Radhakrishna Murthy I. V., Polinaidu B. and Rao A. T. (1991) Magnetic anomalies and basement structures around Vizianagaram, Andhra Pradesh. J. Geol. Sot. India 37, 272-986.
55. Rajendra Prasad, B., Kesava Rao, G., Mall, D.M., Koteswara Rao, P., Raju, S., Reddy, M.S., Rao, G.S.P., Sridher, V., Prasad, A.S.S.S.R.S., 2007. Tectonic implications of seismic reflectivity pattern observed over the Precambrian Southern Granulite Terrain, India. Precambrian Research 53, 1–10.
56. Rao A. T., Rao J. U. and Yoshida M. (1993) Geochemistry and tectonic evolution of the pyroxene granulites from Visakhapatnam in the Eastern Ghat granulite belt, India. J. Geosci. (Osaka City University) 36, 135-150.
57. Sajeev, K., Osanai, Y., Santosh, M., 2004. Ultrahigh-temperature metamorphism followed by two-stage decompression of garnet-orthopyroxene-sillimanite granulites from Ganguvarpatti, Madurai Block, southern India. Contrib. Mineral. Petrol. 148, 29–46.
58. Sajeev, K., Windley, B.F., Connolly, J.A.D., Kon, Y., 2009. Retrogressed eclogite (20 kbar, 1020 C) from the Neoproterozoic Palghat–Cauvery suture zone, southern India. Precambrian Research 171, 23–36.
59. Samuel, V.O., Santosh, M., Liu, S.W., Wang, W., Sajeev, K., 2014. Neoarchean continent growth through arc magmatism in the Nilgiri Block, southern India. Precambrian Res. 245, 146–173.
60. Santosh, M., Maruyama, S., Sato, K., 2009. Anatomy of a Cambrian suture in Gondwana: Pacific-type orogeny in the southern India? Gondwana Res. 16, 321–341.
61. Santosh, M., Morimoto, T., Tsutsumi, Y., 2006. Geochronology of the khondalite belt of Trivandrum Block, Southern India: electron probe ages and implications for Gondwana tectonics. Gondwana Res. 9, 261–278.
62. Santosh, M., Yang, Q.Y., Shaji, E., Ram Mohan, M., Tsunogae, T., Satyanarayanan, M., 2016. Oldest rocks from Peninsular India: evidence for Hadean to Neoarchean crustal evolution. Gondwana Res. 29, 105–135.
63. Santosh, M., Yang, Q.Y., Shaji, E., Tsunogae, T., Ram Mohan, M., Satyanarayanan, M., 2015. An exotic Mesoarchean micro continent: the Coorg Block, southern India. Gondwana Res. 27, 165–195.
64. Santosh, M., Yokoyama, K., Sekhar, S.B., Rogers, J.J.W., 2003. Multiple tectonothermal events in the granulite block of southern India revealed from EPMA dating: implications on the history of supercontinents. Gondwana Res. 6, 29–63.
65. Sato, K., Santosh, M., Tsunogae, T., Chetty, T.R.K., Hirata, T., 2011. Subduction– accretion–collision history along the Gondwana suture in southern India: a laser ablation ICP-MS study of zircon chronology. Journal of Asian Earth Sciences 40, 162–171.
66. Sen S. K. (1987) Origin of leptynites, an orthopyroxene-free granite gneiss, in two granulite terranes of India. In Recent Researches in Geology (edited by Saha A. K.), pp. 117-124. Hindustan, Publishing Corporation, Delhi.
67. Sengupta P., Dasgupta S. N., Bhattacharya P. K., Fukuoka M., Chakraborthy S. and Bhowmik S. (1990) Petrotectonic imprints in the sapphirine granulites from Ananthagiri, Eastern Ghat mobile belt, India. J. Petrol. 31, 971-976.
68. Shaji, E., Santosh, M., He, X.F., Fan, H.R., Dhanil Dev, S.G., Yang, K.F., Thangal, M.K., Pradeepkumar, A.P., 2014. Convergent margin processes during Archean–Proterozoic transition in

ISSN No. 2321-2705 | DOI: 10.51244/IJRSI |Volume XII Issue VII July 2025

southern India: geochemistry and Zircon U–Pb geochronology of goldbearing amphibolites, associated metagabbros, and TTG gneisses from Nilambur. Precambrian Res. 250, 68–96.
69. Shaw D. M. (1968) A review K-Rb fractionation trends by covariance analysis. Geochim. Cosmochim. Acta 32, 573-601.
70. Sriramadas A. and Rao A. T. (1979) Charnockites of Visakhapatnam, Andhra Pradesh. J. Geol. Sot. India 20, 512-517. Subramaniam A. P. (1959) Charnockites of the type area Madras-a reinterpretation. American J. Sci. 257, 321-353.
71. Tateishi, K., Tsunogae, T., Santosh, M., Janardhan, A.S., 2004. First report of sapphirine + quartz assemblage from southern India: implications for ultrahigh temperature metamorphism. Gondwana Res. 7, 899–912
72. Taylor S. R. and McLennan S. M. (1981) The composition and evolution of continental crust: rare earth element evidence from continental rocks. Phil. Trans. R. Sot. (London) A301, 381-399.
73. Taylor S. R. and McLennan S. M. (1985) The Continental Crust: Its Composition and Evolution. Blackwell, Oxford, 312 pp.
74. Tomson, J.K., Bhaskar Rao, Y.J., Vijaya Kumar, T., Mallikharjuna Rao, J., 2006. Charnockite genesis across the Archaean–Proterozoic terrane boundary in the South Indian Granulite Terrain: constraints from major-trace element geochemistry and Sr–Nd isotopic systematics. Gondwana Research 10, 115–127.
75. Tsunogae, T., Santosh, M., 2011. Sapphirine + quartz assemblage from the Southern Granulite Terrane, India: diagnostic evidence for ultrahigh-temperature metamorphism within the Gondwana collisional orogen. Geol. J. 46, 183–197.
76. Venkateswara Rao V., Radhakrishna Murthy I. V. and Rao A. T. (1990) Magnetic anomalies and tectonics of Gosthani River basin in the Eastern Ghats of India. J. Geol. Sot. India 35, 287-295.
77. Viswanathan T. V. (1969) The granulite rocks of the Indian Precambrian Shield. Geological Survey of India Memoir, (Published by Geological Survey of India), Calcutta. Geol. Surr. India Mem. 100, 37-66.
78. Waters D. J. (1988) Partial melting and formation of granulite facies assemblage in Namaqualand, South Africa. J. Metamorph. Geol. 6, 387-404.
79. Wernick E. and De Almeida P. F. M. (1979) The geotectonic environments of early Precambrian granulites in Brazil. Precambrian Res. 8, l-17.
80. Wilson A. F. (1976) Aluminium in coexisting pyroxenes as a sensitive indicator of changes in metamorphic grade within the mafic granulite terrane of the Fraser Range, Western Australia. Contrib. Mineral. Petrol. 56, 255277.
81. Wronkiewicz D. J. and Condie K. C. (1989) Geochemistry of sediments from the Pongola super group, South Africa, evidence for a 3 Ga old evolved continental craton. Geochim. Cosmochim. Acta 53, 1537-1549.
82. Yang, Q.Y., Santosh, M., Pradeepkumar, A.P., Shaji, E., Prasanth, R.S., Dhanil Dev, A.G., 2015. Crustal evolution in the western margin of the Nilgiri Block, southern India: insights from zircon U–Pb and Lu–Hf data on Neoarchean magmatic suite. J. Asian Earth Sci. 113, 766–777.